Decomposition of Rare Earth Loaded Resin Particles – Fiscal Year 2010

Stewart Voit[1], Ilir Beta[2], Claudia Rawn[1]
(1) Oak Ridge National Laboratory
(2) Netzsch Instruments Boston, Thermoanalytical Section

1 Introduction

The Fuel Cycle R&D (FCR&D) program within the Department of Energy Office of Nuclear Energy (DOE-NE) is evaluating nuclear fuel cycle options, including once-through, modified open, and fully closed cycles. Each of these scenarios may utilize quite different fuel management schemes and variation in fuel types may include high thermal conductivity UO_2, thoria-based, TRISO, metal, advanced ceramic (nitride, carbide, composite, etc.), and minor actinide (MA) bearing fuels and targets.

Researchers from the U.S., Europe, and Japan are investigating methods of fabricating high-specific activity spherical particles for fuel and target applications. The capital, operating, and maintenance costs of such a fuel fabrication facility can be significant, thus fuel synthesis and fabrication processes that minimize waste and process losses, and require less footprint are desired. Investigations have been performed at the Institute for Transuranium Elements (ITU) and the French Atomic Energy Commission (CEA) studying the impact of americium and curium on the fuel fabrication process. Proof of concept was demonstrated for fabrication of MA-bearing spherical particles, however additional development will be needed for engineering scale-up.[i] Researchers at the Paul Scherer Institute (PSI) and the Japan Atomic Energy Association (JAEA) have collaborated on research with ceramic-metallic (CERMET) fuels using spherical particles as the ceramic component dispersed in the metal matrix.[ii] Recent work at the CEA evaluates the burning of MA in the blanket region of sodium fast reactors.[iii] There is also interest in burning MA in Canada Deuterium Uranium (CANDU) reactors.[iv] The fabrication of uranium-MA oxide pellets for a fast reactor blanket or MA-bearing fuel for CANDU reactors may benefit from a low-loss dedicated footprint for producing MA-spherical particles.

One method for producing MA-bearing spherical particles is loading the actinide metal on a cation exchange resin. The AG-50W resin is made of sulfonic acid functional groups attached to a styrene divinylbenzene copolymer lattice (long chained hydrocarbon). The metal cation binds to the sulfur group, then during thermal decomposition in air the hydrocarbons will form gaseous species leaving behind a spherical metal-oxide particle. Process development for resin applications with radioactive materials is typically performed using surrogates. For americium and curium, a trivalent metal like neodymium can be used.

Thermal decomposition of Nd-loaded resin in air has been studied by Hale.[v] Process conditions were established for resin decomposition and the formation of Nd_2O_3 particles. The intermediate product compounds were described using x-ray diffraction (XRD) and wet chemistry. Leskela and Niinisto studied the decomposition of rare earth (RE) elements and found results consistent with Hale.[vi] Picart et al. demonstrated the viability of using a resin loading process for the fabrication of uranium-actinide mixed oxide microspheres for transmutation of minor actinides in a fast reactor.[vii]

For effective transmutation of actinides, it will be desirable to extend the in-reactor burnup and minimize the number of recycles of used actinide materials. Longer burn times increases the chance of Fuel Clad Chemical or Mechanical Interaction (FCCI, FCMI). Sulfur is suspected of contributing to Irradiation Assisted Stress Corrosion Cracking (IASCC)[viii,ix] thus it is necessary to maximize the removal of sulfur during decomposition of the resin.

The present effort extends the previous work by quantifying the removal of sulfur during the decomposition process. Neodymium was selected as a surrogate for tri-valent actinide metal cations. As described above Nd was dissolved in nitric acid solution then contacted with the AG-50W resin column. After washing the column, the Nd-resin particles are removed and dried. The Nd-resin, seen in Figure 1 prior to decomposition, is ready to be converted to Nd oxide microspheres.

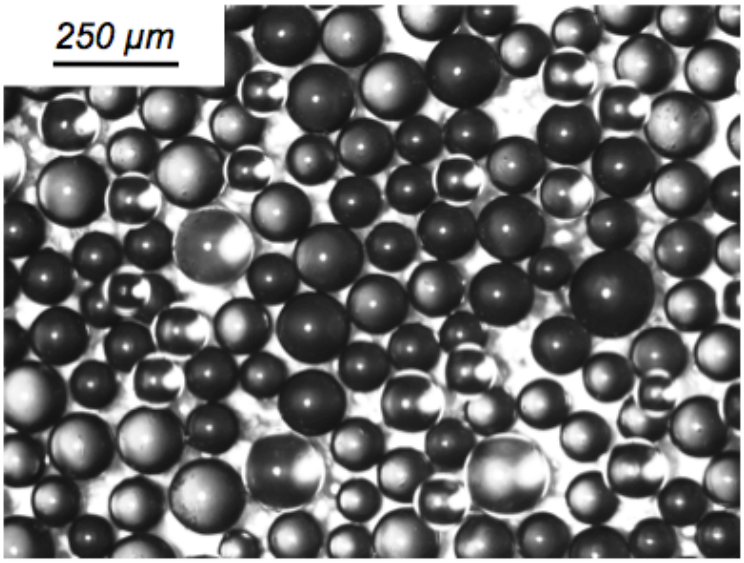

Fig. 1: Neodymium-loaded AG-50W resin particles.

2 Thermal Decomposition of Nd-Loaded Resin

Several attempts were made to quantify the sulfur removal during decomposition. The first run was aimed at establishing a baseline for sulfur removal by duplicating the decomposition in air demonstrated by Hale. Subsequent runs attempted to

improve on sulfur removal by the use of hydrogen in the process gas stream. A NETZSCH Simultaneous Thermal Analyzer (STA) 449 F1 Jupiter was used to measure the mass change and transformation energetics during decomposition. The evolved gases were analyzed with a NETZSCH Quadrupole Mass Spectrometer (QMS) 403 Aeolos system coupled to the STA by means of a transfer line which was kept at a constant temperature of 250°C. The mass spectrometer of the QMS 403 was programmed to detect mass numbers between 1 and 100 amu, ignoring mass numbers greater than 100 amu.

Samples were also processed in a furnace using temperature and atmosphere conditions identical to the STA runs and samples were taken at discrete points during the decomposition process and sent for analytical chemistry in order to quantify the sulfur content.

2.1 Decomposition in air at 1400°C

The first run of Nd-loaded resin in air was performed under the following conditions:

- Ramp rate: 5°C per minute
- Atmosphere: air
- Isothermal hold: 1400°C
- Hold time: 1 hour

The Thermogravimetry (TG), Derivative Thermogravimetry (DTG) and Differential Scanning Calorimetry (DSC) curves are plotted in Figure 2. The TG curve shows six mass loss steps of 10.72%, 11.48%, 12.91%, 43.20%, 2.86% and 3.56%. The first, second, third, fifth and sixth mass loss steps have corresponding peaks at 125.9°C, 348.0°C, 467.5°C, 871.5°C and 1284.9°C, whereas the fourth mass loss step is a convolution of two sub-steps with corresponding peaks at 564.0°C and 659.4°C in the DTG curve. The DSC curve initially shows an endothermic peak at 121.3°C which correspond with the first mass loss step and is probably due to evaporation of moisture from the sample. At higher temperatures the DSC curve shows two exothermic peaks at 458.8°C and 726.4°C, which both have shoulders on the low-temperature side, and are due to the oxidation of the organic material in air. Two small endothermic peaks at 875.3°C and 1286.6°C correspond with the fifth and sixth mass loss steps and are due to decomposition processes.

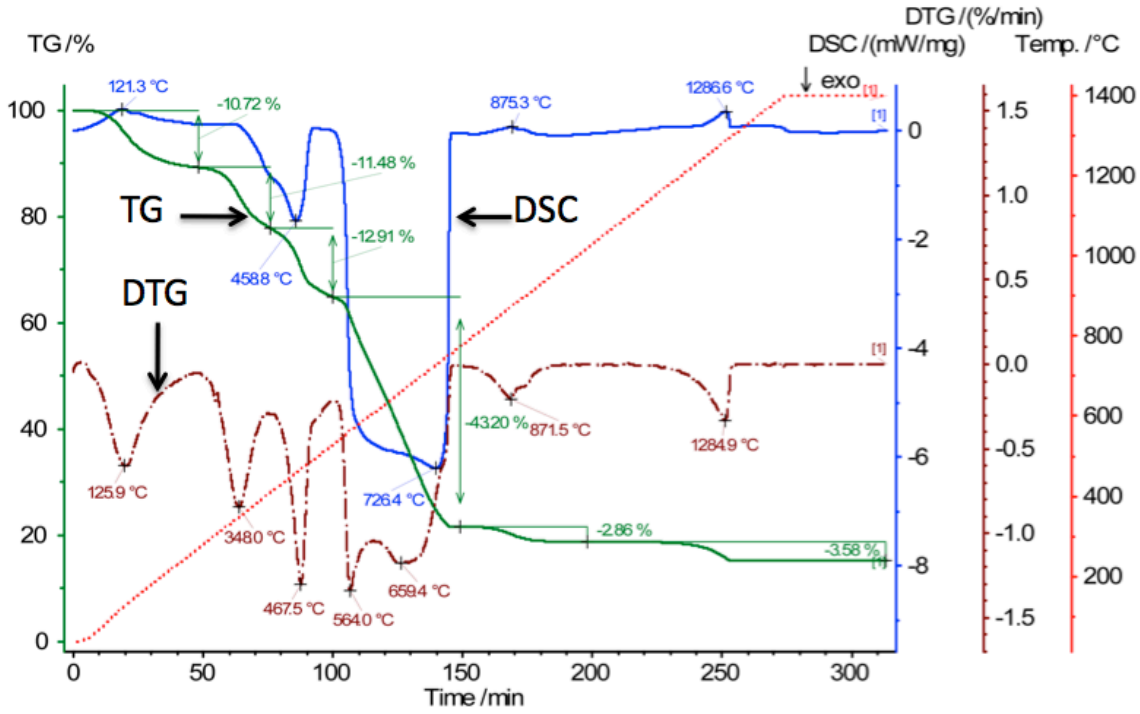

Fig. 2. TG, DTG and DSC curves for Nd-loaded AG-50W resin in air.

The QMS ion-current curves for H_2O (17; 18 amu), CO_2 (12; 44 amu) and SO_2 (48; 64 amu) are plotted in Figures 3 and 4 along with the TG curve. As can be clearly seen from Figure 3, H_2O is evolved primarily in three steps: the first and the third steps correspond to the peaks at 128.3°C and 561.3°C while the second step has a main peak at 464.8°C and two smaller peaks at 347.7°C and 388.6°C in the 18 amu ion-current curve. CO_2 release occurs at relatively high temperatures with a small peak at 464.8°C and a much larger peak at 674.8°C in the 44 amu ion-current curve. Figure 4 clearly shows that SO_2 is evolved in five steps which have corresponding peaks at 348.6°C, 457.8°C, 647.4°C, 865.2°C and 1274.0°C in the 48 amu ion-current curve.

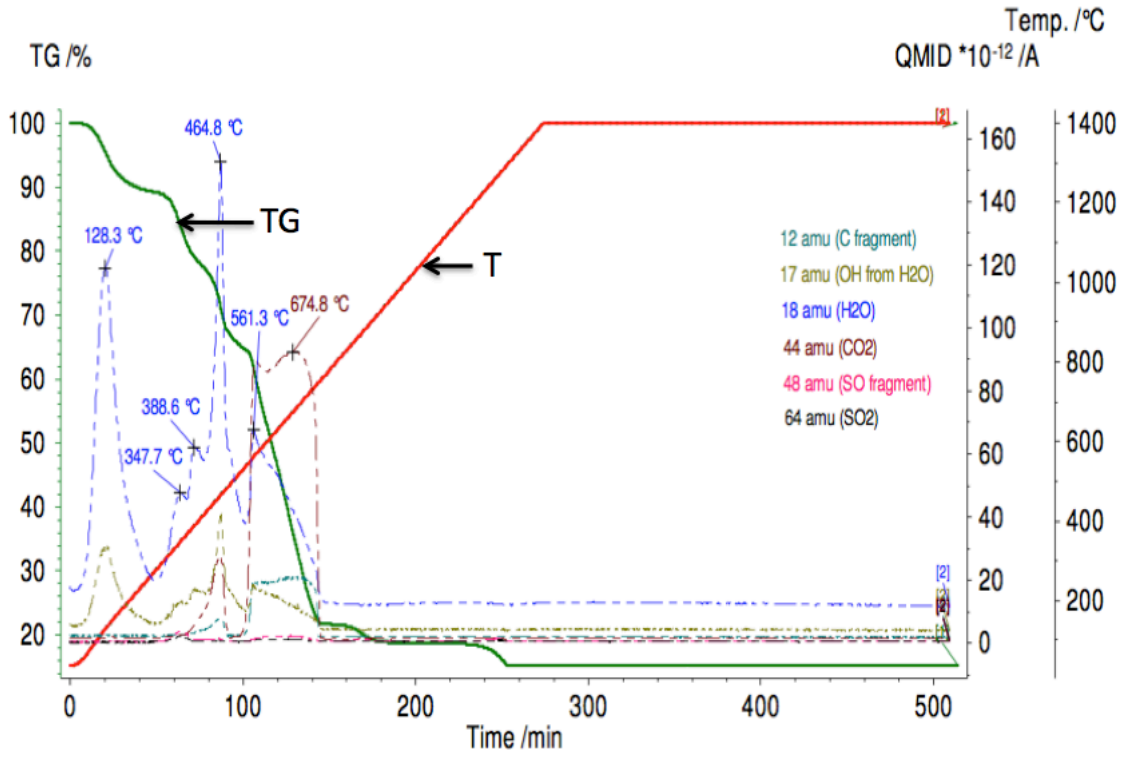

Fig. 3. QMS ion-current curves for the 12; 17; 18; 44; 48 and 64 amu mass numbers and TG curve for Nd-loaded AG-50W resin in air.

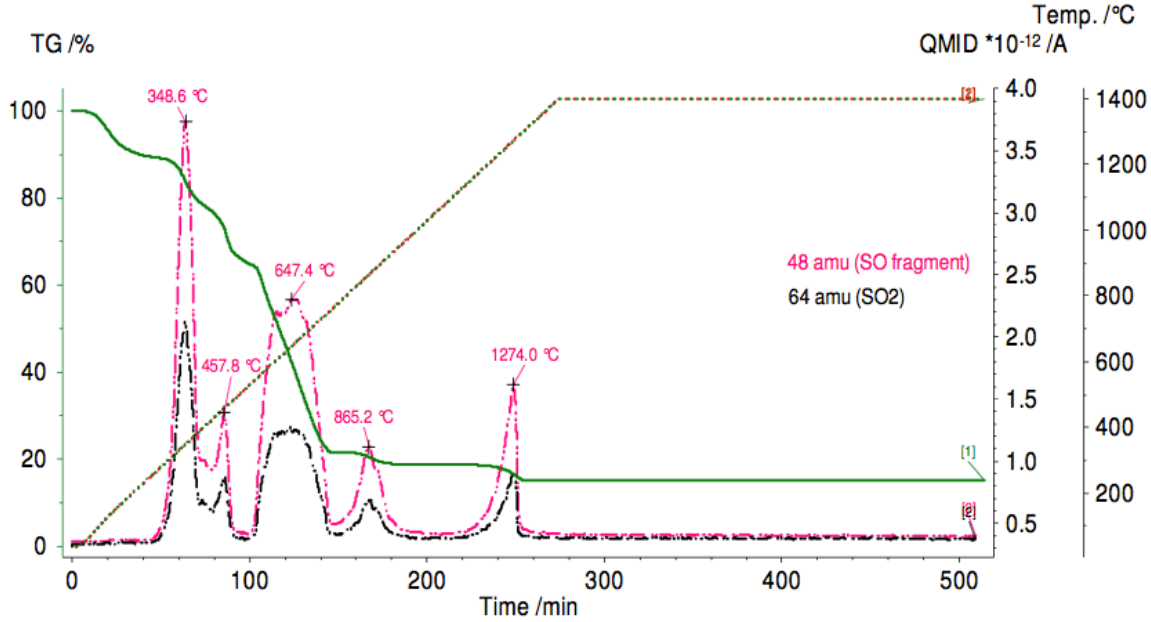

Fig. 4: QMS ion-current curves for the 48 and 64 amu mass numbers and TG curve for Nd-loaded AG-50W resin in air.

2.2 Decomposition in Ar-6%H_2 up to 500°C followed by air up to 1400°C

When loading a metal cation (in this case Nd) on the resin, the loading efficiency is never 100%, therefore a fraction of the sulfonic acid groups remain unbound. The next experiment introduced hydrogen gas during the dehydration stage of the thermal treatment in an attempt to more effectively remove the unbound sulfur before the resin matrix begins to decompose. The processing conditions for this run are as follows:

- Ramp rate: 5°C per minute
- Atmosphere: Ar-6%H_2 gas
- Isothermal hold: 500°C
- Switch to Ar gas
- Hold time: 30 minutes
- Switch to air
- Ramp rate: 5°C per minute
- Atmosphere: air
- Isothermal hold: 1400°C
- Hold time: 1 hour

The TG, DTG and DSC curves are plotted in Figure 5. The TG curve shows six mass loss steps of 11.25%, 10.42%, 15.27%, 37.08%, 2.95% and 3.29%. The first, second, third, fifth and sixth mass loss steps have corresponding peaks at 102.6°C, 347.3°C, 476.3°C, 843.4°C and 1256.0°C while the fourth mass loss step is a convolution of three sub-steps with peaks at 505.9°C, 579.6°C and 628.3°C in the DTG curve. The DSC curve shows three endothermic peaks at 106.3°C, 346.6°C and 479.1°C which correspond with the first three mass loss steps, followed by a sharp exothermic peak at 505.3°C and a much larger exotherm at 650.0°C. There are also two small endothermic peaks at 847.5°C and 1254.7°C, which correspond with the fifth and sixth mass loss steps.

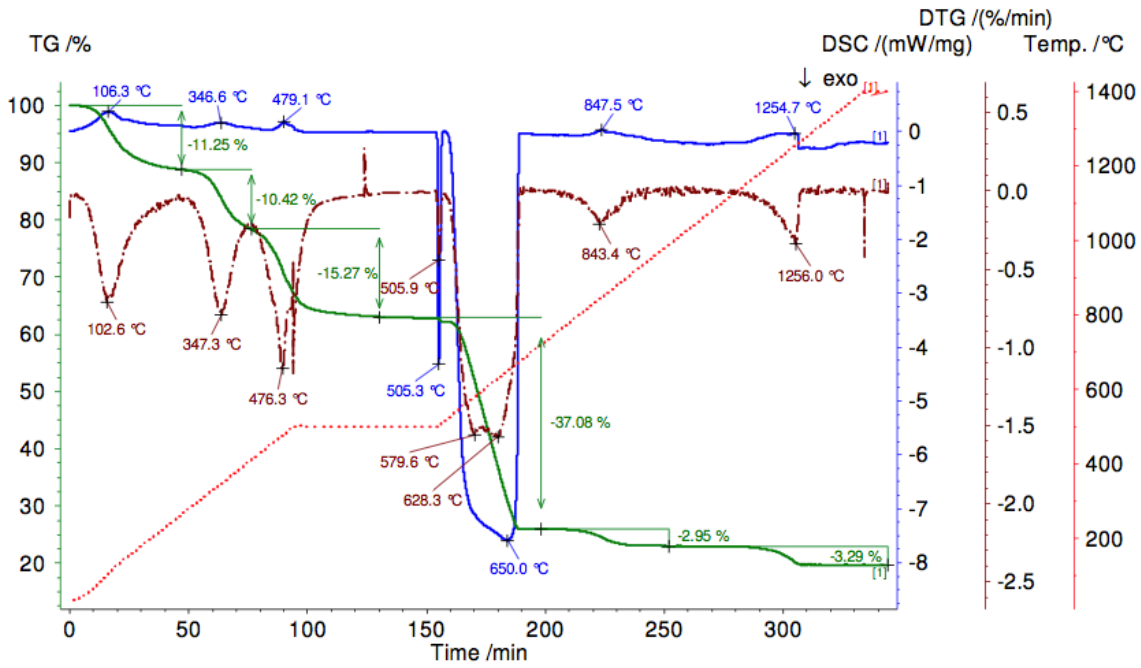

Fig. 5. TG, DTG and DSC curves for Nd-loaded AG-50W resin in Ar-6%H_2 up to 500°C followed by air up to 1400°C.

The QMS ion-current curves of H_2O (17 and 18 amu), CO_2 (12 and 44 amu), CH_4 (16 amu) and the CH_3 methyl fragment (15 amu) are plotted in Figure 6 along with the TG curve. The 17 and 18 amu ion- current curves of H_2O show four peaks at 110.0°C, 343.6°C, 384.5°C and 474.8°C and two additional peaks immediately after switching to air at 500°C and 557.7°C. The 16 amu signal of CH_4 is similar to the ion-current curves of H_2O with slightly shifted peak positions. Methyl fragments are evolved as a peak at 460.6°C in the 15 amu signal. The 12 and 44 amu ion-current curves of CO_2 show a peak at 497.9°C and two other peaks immediately after switching to air at 500°C.

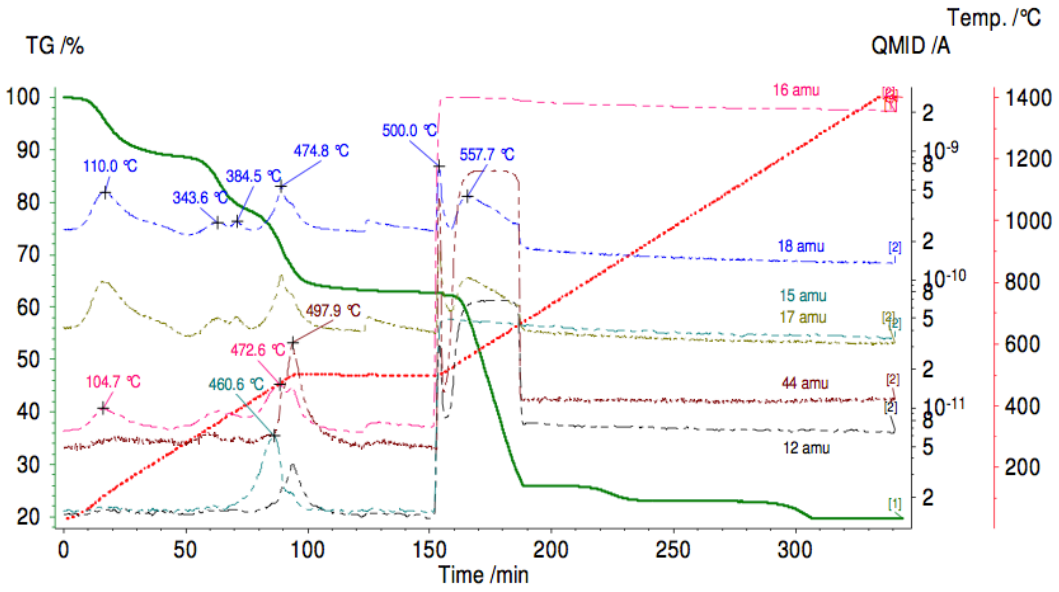

Fig. 6. QMS ion-current curves for the 12; 15; 16; 17; 18 and 44 amu mass numbers and TG curve for Nd-loaded AG-50W resin in Ar-6%H_2 up to 500ºC followed by air up to 1400ºC.

The QMS ion-current curves of elemental sulfur (32 amu), H_2S (33 and 34 amu) and SO_2 (48 and 64 amu) are plotted in Figure 7 along with the TG curve. Elemental sulfur is evolved in three main steps with corresponding peaks at 111.3°C, 345.8°C and 465.0°C in the 32 amu ion-current curve. The 33 and 34 amu signals of H_2S both show one peak at 465.0°C with a shoulder on the low-temperature side. The 48 and 64 amu ion-current curves of SO_2 show six main peaks at 345.8°C, 491.3°C, 500.3°C, 621.9°C, 837.4°C and 1238.5°C.

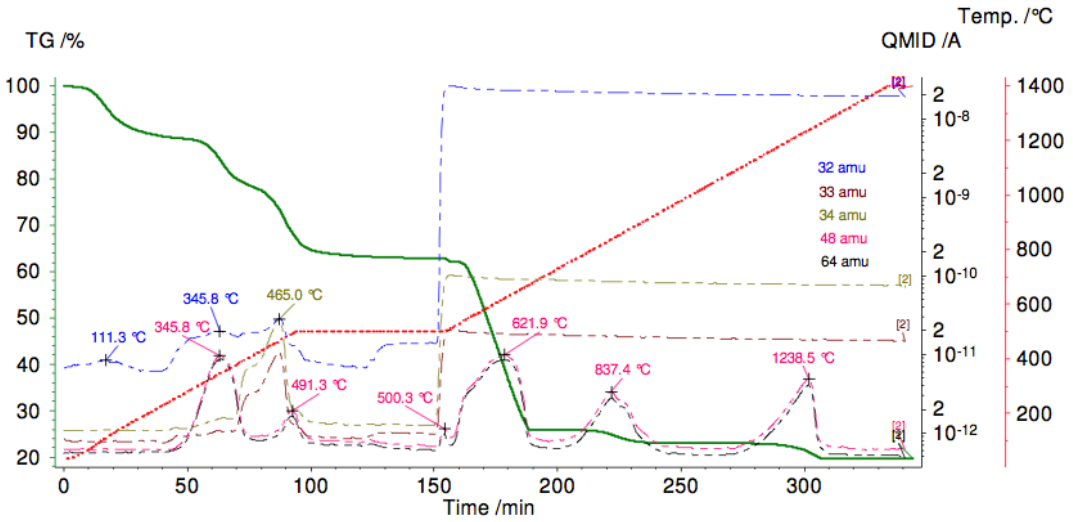

Fig. 7. QMS ion-current curves for the 32; 33; 34; 48 and 64 amu mass numbers and TG curve for Nd-loaded AG-50W resin in Ar-6%H_2 up to 500°C followed by air up to 1400°C.

2.3 Decomposition in Ar-6%H_2 up to 750°C followed by air up to 1400°C

In the next experiment, introduction of hydrogen gas was extended up to the 750°C to determine the effect on decomposition. The processing conditions for this run are as follows:

- Ramp rate: 5°C per minute
- Atmosphere: Ar-6%H_2 gas
- Isothermal hold: 750°C
- Switch to Ar gas
- Hold time: 30 minutes
- Switch to air
- Ramp rate: 5°C per minute
- Atmosphere: air
- Isothermal hold: 1400°C
- Hold time: 1 hour

The resulting TG, DTG and DSC curves are plotted in Figure 8. The TG curve shows five mass loss steps of 12.12%, 10.69%, 20.60%, 36.04% and 3.12%. The first, second, fourth and fifth mass loss steps have corresponding peaks at 106.4°C, 348.9°C, 803.9°C and 1258.1°C, whereas the third mass loss step is a convolution of two sub-steps with corresponding peaks at 476.9°C and 503.1°C in the DTG curve. The DSC curve initially shows three endothermic peaks at 106.9°C, 346.4°C and 479.1°C which correspond with the first three mass loss steps. Upon switching to air at 750°C, a very large exothermic peak at 769.4°C appears in the DSC curve due to oxidation of organic material and carbonaceous residue. Another small exothermic peak at 1272.9°C corresponds with the fifth mass loss step in the TG curve.

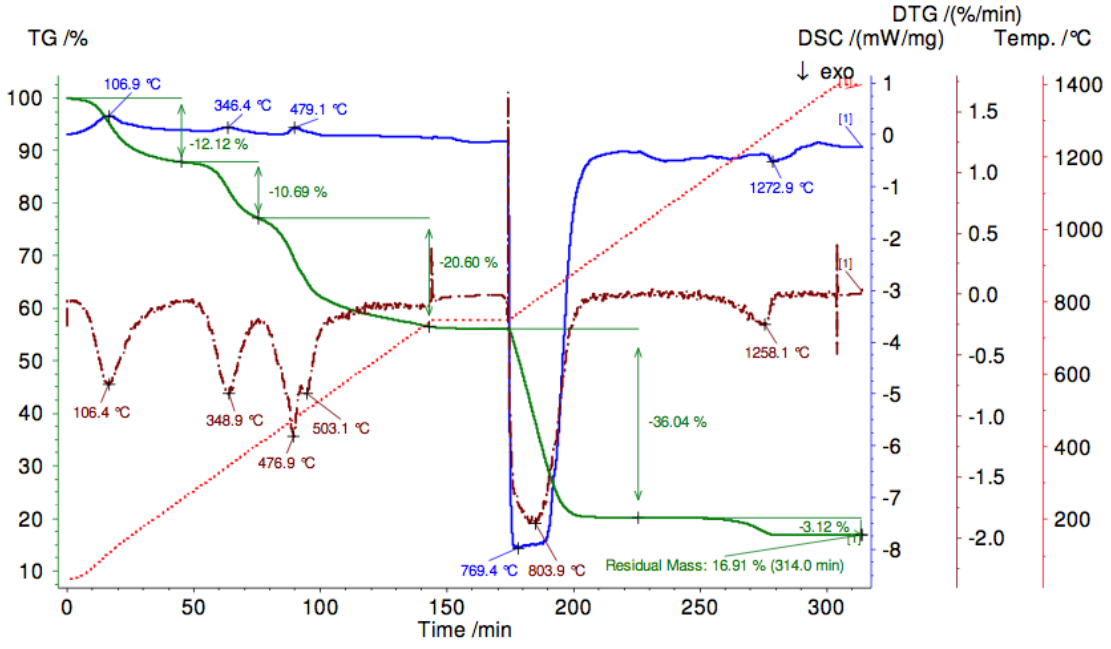

Fig. 8. TG, DTG and DSC curves for Nd-loaded AG-50W resin in Ar-6%H_2 up to 750°C followed by air up to 1400°C.

The QMS ion-current curves of H_2O (17 and 18 amu), CO_2 (12 and 44 amu), CH_4 (16 amu) and the methyl fragment (15 amu) are plotted in Figure 9 along with the TG curve. The 17 and 18 amu ion-current curves of H_2O show four peaks at 108.5°C, 345.5°C, 384.0°C and 474.8°C and an additional sharp peak immediately after switching to air at 750°C. The 16 amu signal of CH_4 is very similar to the ion-current curves of H_2O, but shows an additional peak at about 670°C. Methyl fragments are evolved in two steps with corresponding peaks at 460.6°C and 669.7°C in the 15 amu signal. The 12 and 44 amu ion-current curves of CO_2 show a peak at 500.0°C and another much larger peak immediately after switching to air at 750°C.

The QMS ion-current curves of elemental sulfur (32 amu), H_2S (33 and 34 amu) and SO_2 (48 and 64 amu) are plotted in Figure 10 along with the TG curve. Elemental sulfur is evolved in three main steps with corresponding peaks at 103.1°C, 345.5°C and 468.2°C in the 32 amu ion-current curve. The 33 and 34 amu signals of H_2S show one peak at 468.2°C with a shoulder on the low-temperature side. The 48 and 64 amu ion-current curves of SO_2 show three main peaks at 348.8°C, 807.9°C and 1241.4°C and a smaller feature at about 470°C.

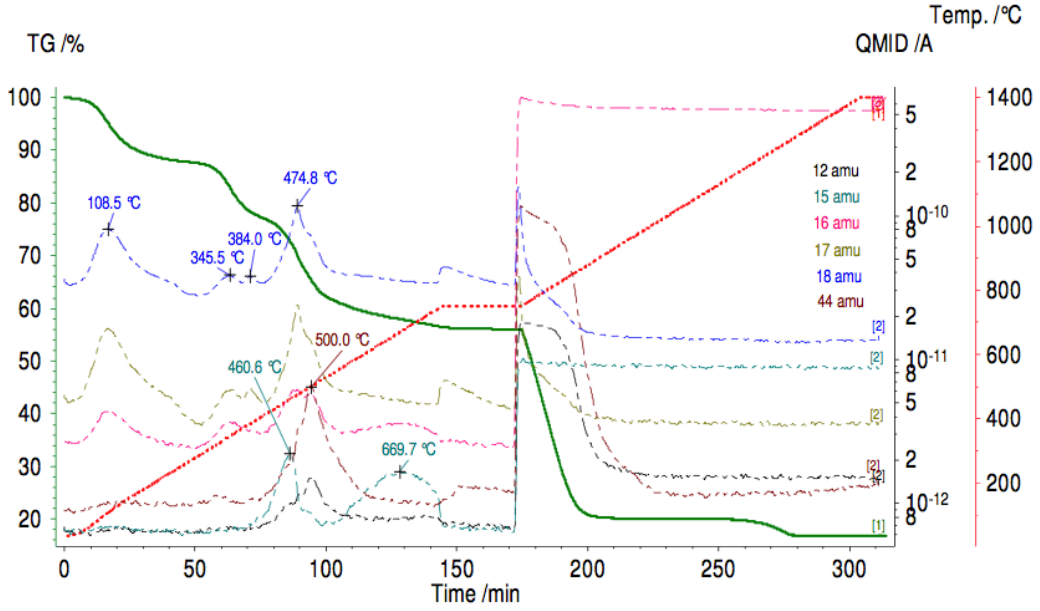

Fig. 9. QMS ion-current curves for the 12; 15; 16; 17; 18 and 44 amu mass numbers and TG curve for Nd-loaded AG-50W resin in Ar-6%H_2 up to 750°C followed by air up to 1400°C.

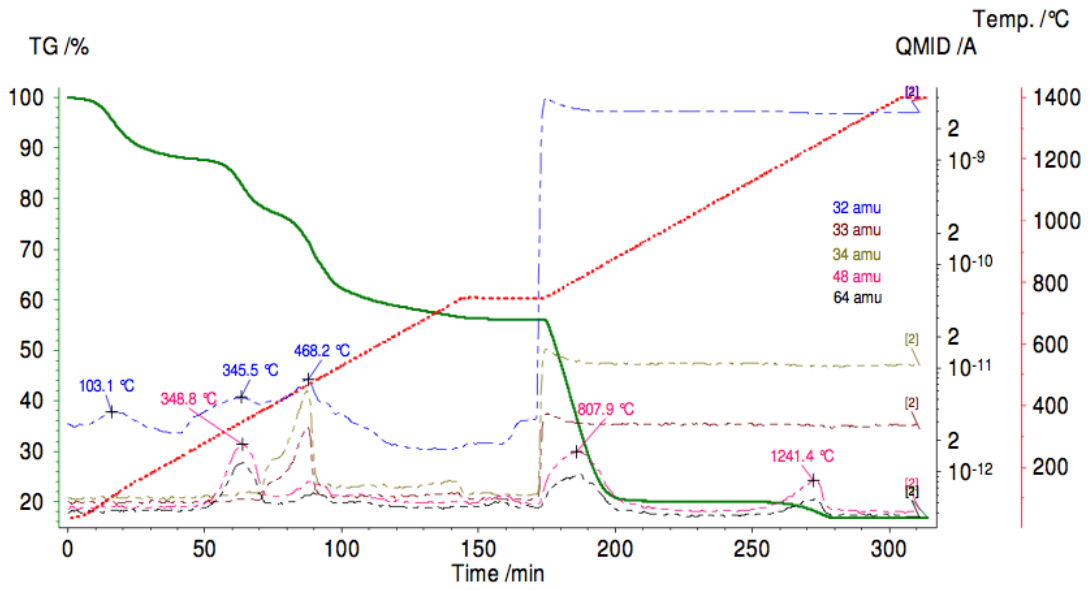

Fig. 10. QMS ion-current curves for the 32; 33; 34; 48 and 64 amu mass numbers and TG curve for Nd-loaded AG-50W resin in Ar-6%H_2 up to 750°C followed by air up to 1400°C.

3 Sulfur Determination via Analytical Chemistry

Analytical chemistry was used to quantify the amount of elemental sulfur in resin samples taken from discrete points during the decomposition process. Resin samples were processed in a tube furnace under time, temperature, and atmosphere conditions identical to the STA runs. A reference sample of untreated resin was measured to determine the amount of sulfur prior to decomposition. For the three STA runs described in Sections 2.1, 2.2, and 2.3, four sulfur values are presented; (1) the reference value, (2) prior to the decomposition endotherm, (3) after the endotherm, and (4) after completion of the run. A visual example of the sampling scheme is shown in Figure 11 and a comparison of the results for the three runs is presented in Figure 12 and in tabular format in Table 1.

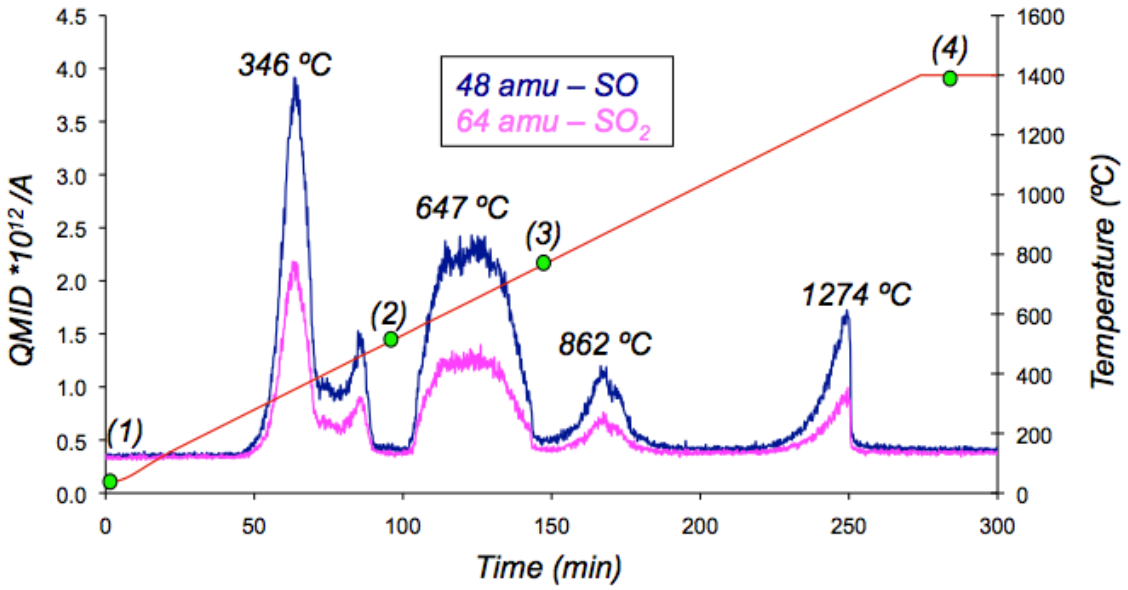

Fig. 11: Four sampling points for sulfur determination via analytical chemistry.

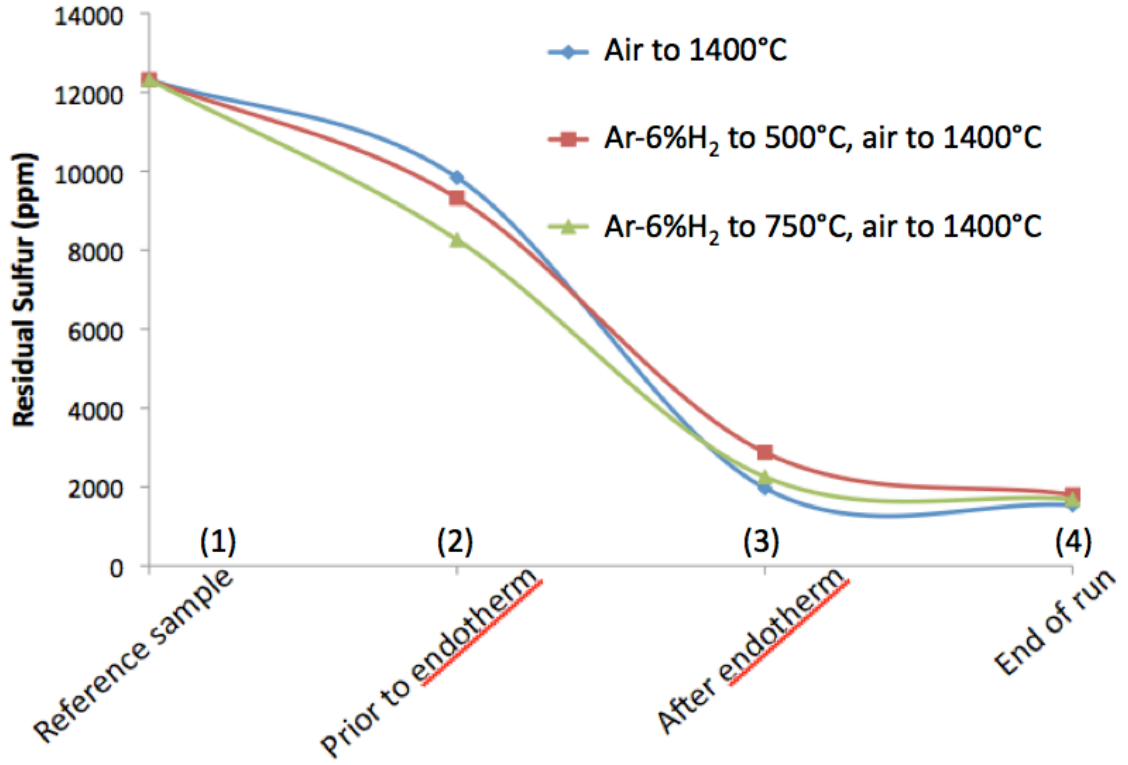

Fig. 12: Amount of residual sulfur measured using analytical chemistry at four sample points corresponding to each STA run.

Table 1. Sulfur value (ppm) for four sample points corresponding to each STA run

Sample No.	Air to 1400ºC	Ar-6%H_2 to 500ºC, air to 1400ºC	Ar-6%H_2 to 750ºC, air to 1400ºC
1	12320	12320	12320
2	8263	9321	9840
3	1970	2875	2256
4	1540	1800	1690

4 X-Ray Diffraction

XRD was used to confirm the phase content of the resin during decomposition. It would be instructive to study the phase changes by collecting in-situ diffraction data as a function of temperature. This can be done using a hot-stage XRD where the sample is placed on a platinum heater strip and the strip is raised to temperature through resistance heating.

The first attempt at collecting in-situ diffraction was not completely successful. Figure 13 displays an overlay of diffraction patterns taken at three different temperatures; 25°C, 800°C, and 1400°C. The temperatures correspond to the reference resin, after the endotherm, and after run completion respectively. The pattern at 25°C has two distinct features. The first is the presence of two prominent peaks that correspond to the platinum heater strip. The second is the completely amorphous background with the only crystalline structure associated with the platinum.

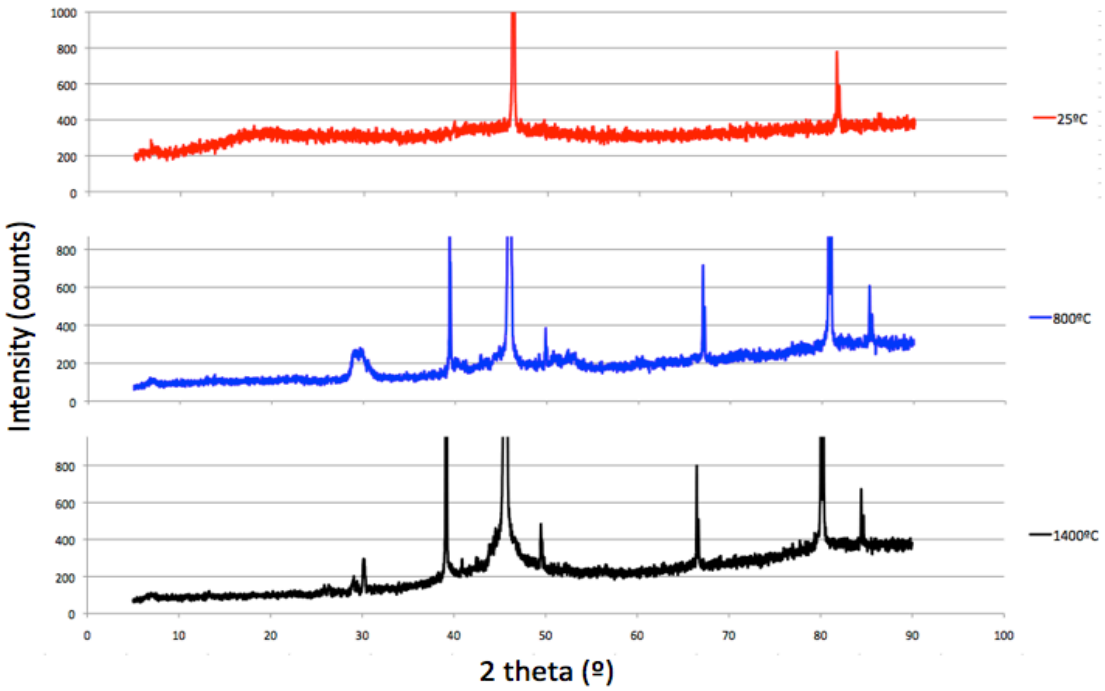

Fig. 13. Resin sample on hot stage XRD platinum heater strip.

The pattern at 800°C indicates the presence of an undetermined Nd-oxysulfide compound and at 1400°C, the results suggest the formation of Nd_2O_3. It was not possible to quantify the phase composition at these temperatures due to the very low peak intensity/background ratio. Part of the problem resulted from an extreme morphology change in the sample during heating. Figure 14 shows a picture of the sample on the platinum heater strip after the first run. Before the run, the resin sample was placed on the heater strip in a uniform layer. During decomposition, the resin undergoes a significant volume reduction and in addition, Figure 14 shows how the edges of the sample curled up. These physical changes affect sample surface displacement and distorts the XRD pattern making it very difficult to refine the data and quantify the phase content.

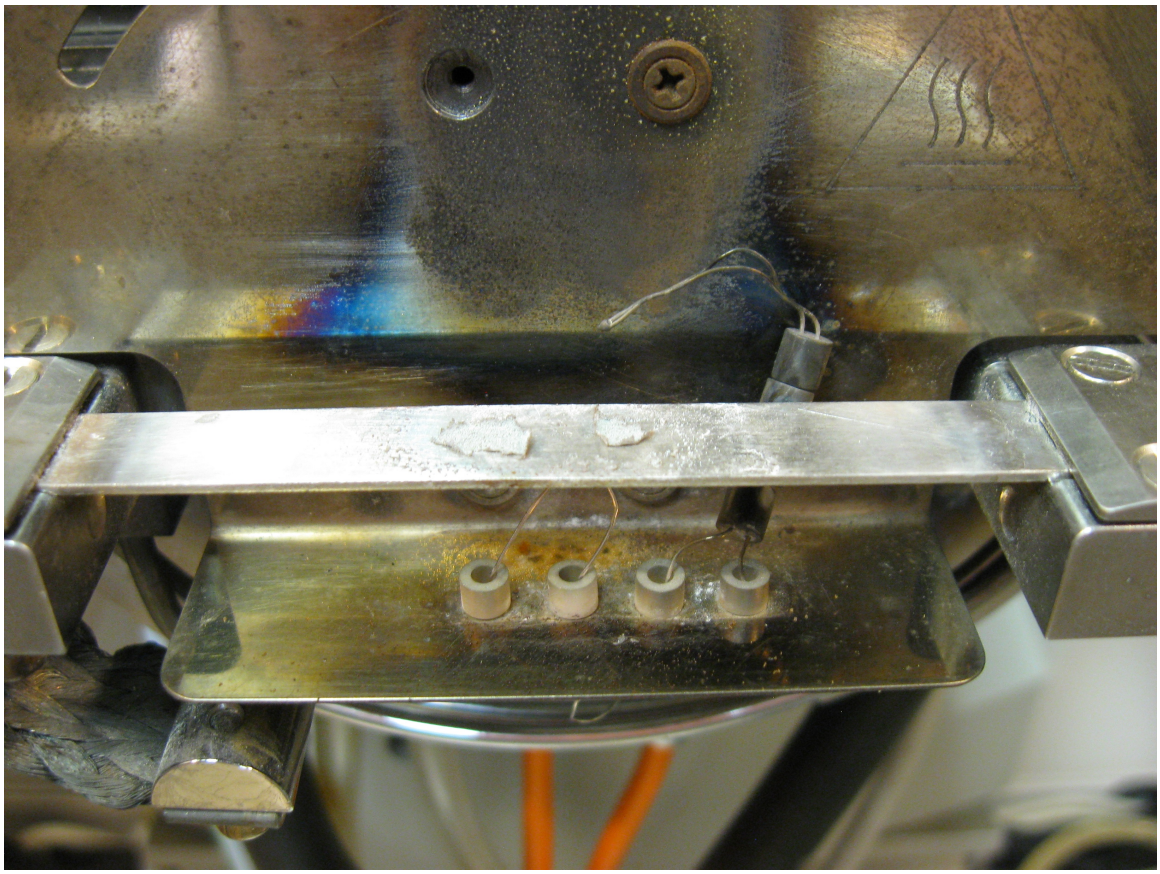

Fig. 14. Resin sample on hot stage XRD platinum heater strip.

The methodology for performing in-situ XRD measurements of the resin decomposition needs additional development work so XRD was performed on a sample taken after a furnace run to 1400°C in air. The results shown in Figure 15 indicate a good match with the Inorganic Crystal Structure Database (ICSD) card for Nd_2O_3.

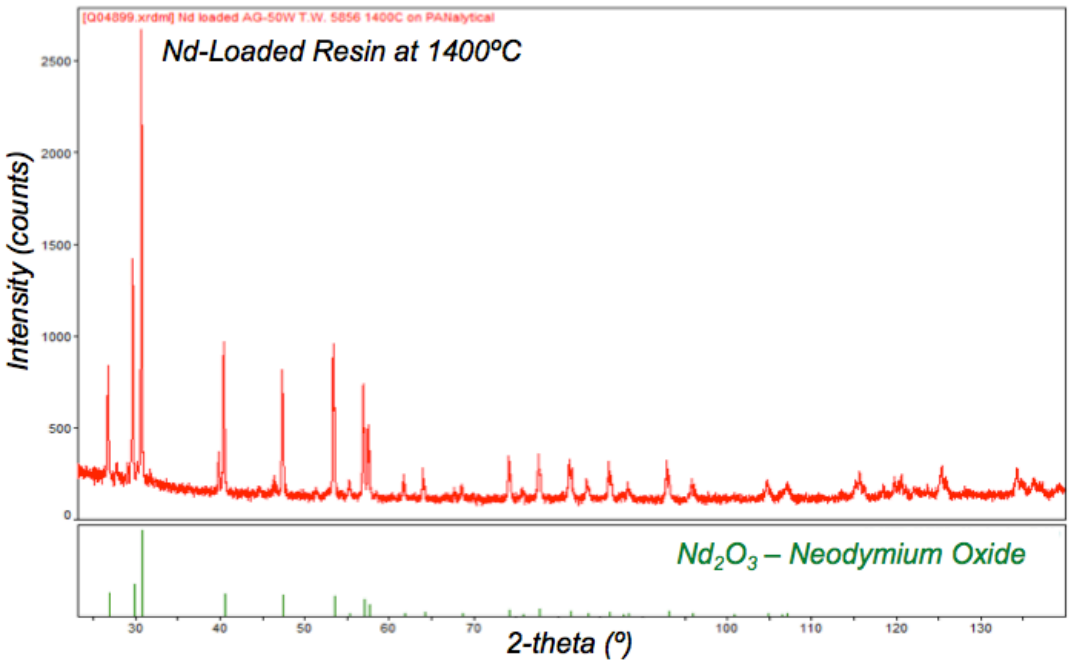

Fig. 15. XRD results for Nd-loaded resin in air at 1400°C.

5 Discussion

The use of hydrogen to assist with sulfur removal at the early stages of decomposition may be beneficial. When comparing sample total weight loss values (see Table 2) for the three STA runs with sulfur loss data from Table 1 (and seen visually in Figure 12), it appears that hydrogen may increase sulfur loss during the dehydration stage.

Table 2. Sample weight loss for the three STA runs as determined by thermogravimetry

STA Run	Weight Loss After Dehydration (%)	Weight Loss During Endotherm (%)	Total Weight Loss (%)
Air to 1400°C	35.1	43.2	84.75
Ar-6%H_2 to 500°C, air to 1400°C	36.94	37.08	80.26
Ar-6%H_2 to 750°C, air to 1400°C	43.41	36.04	83.09

In fact, the hydrogen-assisted sulfur removal during de-hydration may have been prematurely terminated in the STA run in which Ar-6%H_2 was used up to 500°C. This is illustrated by a comparison of Figures 16a and 16b. In these figures, the QMS ion current was plotted versus time for just the volatile sulfur species for the 500°C

case in 16a and the 750°C case in 16b. Because the off-gas analysis was not calibrated, a direct comparison of the ion current magnitude cannot be made.

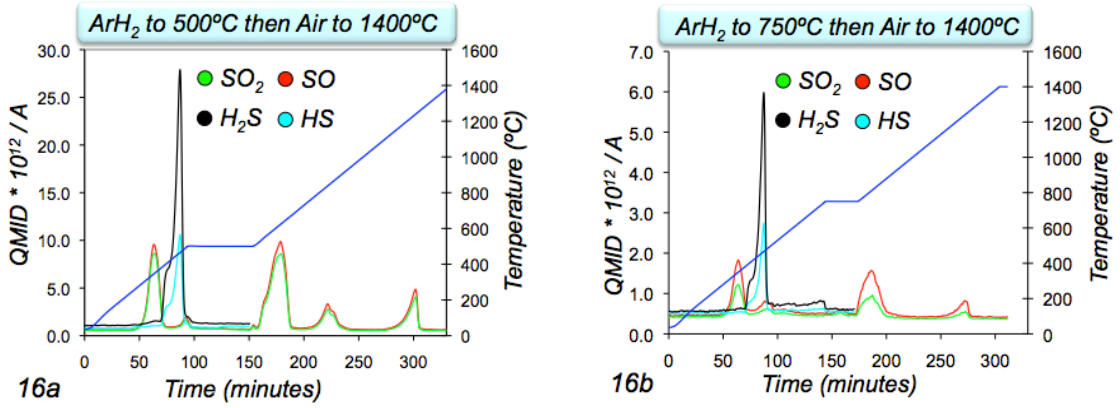

Fig. 16a and 16b. QMS ion current curves for sulfur-bearing compounds evolved from the two argon-hydrogen STA runs.

However in 16a, it can be seen that the concentration of H_2S and HS in the off-gas ceases when the Ar-6%H_2 gas is switched to argon. In the 750°C case, the process gas switch does not occur until well after de-hydration is complete. Comparing the ratio of the first two peak heights for the two cases reveals that hydrogen-assisted sulfur removal can be increases by ~10% by continuous use of the hydrogen-bearing process gas stream until de-hydration is complete.

The maximum sulfur loss however is found when air is used to initiate decomposition after de-hydration is complete. When hydrogen is used at higher temperatures, decomposition is delayed and the endothermic reaction proceeds more energetically compared to air. The shorter reaction time may trap excess carbon and sulfur in the matrix thus lowering the total weight loss and increasing the residual sulfur in the final product. Instead of a constant heat rate, it may be advantageous to have an isothermal hold at 500°C then switch to air followed by a ramp to 1400°C and a longer isothermal hold.

6 Conclusions

Actinides can be loaded on a cation exchange resin, such as AG-50W, for use in various fuel/target configurations to support transmutation fuel cycle options. The particles produced from the resin loading process are spherical with good flowability characteristics and can be considered a near-dustless material form amenable to glovebox or remote transmutation fuel fabrication.

The transmutation of minor actinides may be performed in a nuclear reactor with the actinide-bearing fuel or target form loaded into pins. Sulfur is suspected of contributing to the chemical attack of stainless steel-type fuel pin cladding material,

therefore it is important to minimize the amount of residual sulfur in nuclear fuel or target material that may come in contact with the clad.

The goal of this study was to quantify the evolution of volatile sulfur compounds from Nd-loaded AG-50W resin particles, where Nd is selected as a surrogate for tri-valent actinides. A baseline thermal treatment was carried out in air following a procedure previously established in the literature and the sulfur content at various stages of decomposition was determined. The effect of using a hydrogen-bearing process gas on sulfur removal was studied under varied conditions. The results indicate that a hybrid approach using both hydrogen- and oxygen-assisted sulfur removal may yield improved results. Even at present sulfur levels, resin technology may be used for producing a near-dustless feed material for a fuel/target where the MA concentrations are not more than 10% loading in the matrix.

---

[i] Pillon, S., et al., J. of Nucl. Mater., 320 (2003) 36–43

[ii] Pouchon, M.A., et al., J. of Nucl. Mater., 319 (2003) 37–43

[iii] Buiron and al., "Minor actinides transmutation in SFR depleted uranium radial blanket, neutronic and thermal hydraulic evaluation", Global 2007, Boise, Idaho, September 9-13, (2007)

[iv] Hyland, B., Gihm, B., Proceedings of the 18th International Conference on Nuclear Engineering ICONE18 May 17-21, 2010, Xi'an, China, ICONE18-30123

[v] Hale, W., J. Inorg. Nucl. Chem., 33, (1971) 1227-1232

[vi] Leskela, M., Niinisto, L., J. of Thermal Analysis, 18 (1980) 307-314

[vii] Picart, S., et al., Proceedings of Global 2009 Paris, France, September 6-11, 2009 Paper 9400

[viii] Chung, H., Shack, W., Jan. 31, 2006, ANL Report ID ANL-04/10, OSTI ID: 915725

[ix] Tsukada, T., et al., Proceedings of the Eighth International Symposium on Environmental Degradation of Materials in Nuclear Power Systems – Water Reactors, Vols. 1&2, (1997), 795-802